CHAPTER 6

Recommended Values for Steady-State Atmospheric Lifetimes and their Uncertainties

Lead-Authors:
Malcolm K. W. Ko
Paul A. Newman
Stefan Reimann
Susan E. Strahan

Co-Authors:
Elliot L. Atlas
James B. Burkholder
Martyn Chipperfield
Andreas Engel
Qing Liang
Wahid Mellouki
R. Alan Plumb
Richard S. Stolarski
C. Michael Volk

CHAPTER 6

Recommended Values for Steady-State Atmospheric Lifetimes and Their Uncertainties

Contents

This report assesses the current understanding of processes that control the lifetimes of trace gases in the atmosphere, the ability of models to simulate these processes, and how observations and models are used to provide lifetime estimates. This chapter draws from the results of Chapters 2 to 5 to derive recommended values for the steady-state atmospheric lifetimes of the species listed in Table 1.1. We emphasize that this chapter discusses only findings that have direct implications for the determination of steady-state lifetimes. Readers are urged to look at the summary of each chapter for other findings. We present results and the methodology used to obtain values for the steady-state lifetimes by addressing the following questions:

- **What is new in this reevaluation specific to the issue of steady-state lifetimes?**
- **What methods were used to determine values for steady-state lifetimes?**
- **What are the recommended steady-state lifetimes and uncertainties?**
- **What can be done in future studies to reduce the uncertainties?**

6.1 What Is New in This Reevaluation Specific to the Issue of Steady-State Lifetimes?

In this chapter, we use the term global atmospheric lifetime (GAL) to refer to the lifetime defined as the burden divided by the removal rate from the atmosphere. In the calculation, the burden and the removal rate can be from model simulations or observations. The calculation can be performed for a snap shot in time, or as an average over an annual cycle, or as an average over several years. It is recognized that the GAL takes on different values when the emissions are changing with time. The term steady-state lifetime refers to the GAL calculated when an annually repeated emission pattern is used to sustain the burden, and the removal is balanced by the emission to the extent possible given the inter-annual variability inherent in the atmosphere.

To derive trace gas lifetimes and quantify the associated uncertainties, we must assess the entire theoretical knowledge/understanding, the relevant kinetics and photochemistry, the observations, and the models used to calculate burdens and losses. The most important findings in this report that are relevant to lifetime determination include:

With respect to the definition of lifetimes (see Chapter 2):

- The global atmospheric lifetime is not solely defined by the molecule's photochemistry and kinetics. It also depends on the interaction with the Earth system (atmosphere, land, and ocean), and the emission history.
- Observed concentrations of a species in the atmosphere, along with model calculations, can be used to determine its global atmospheric lifetime for the time period when the observations were taken.
- In theory, the steady-state lifetime of a species depends on the spatial pattern of the surface emissions. However, for the species listed in Table 1.1, the steady-state atmospheric lifetime for all surface emissions can be approximated, to within a few percent, with a single value.
- The steady-state response lifetime is defined as the incremental change in burden in response to an incremental change in emission. It has the unique property in that it provides a measure of the time-integrated change in burden following a pulse emission of the same spatial pattern.
- For the species listed in Table 1.1 (with the exceptions of nitrous oxide (N_2O) and methane (CH_4)), the steady-state response lifetime can be approximated by the steady-

state lifetime because there is no large background concentration in the current atmosphere.

With respect to kinetics and photochemistry (see Chapter 3):

- The dominant loss process for the CFCs, CCl_4, N_2O, CF_3Br (Halon-1301), and NF_3 is photolysis, primarily in the stratosphere in the 190-230 nanometer (nm) wavelength region. For the Halons CF_2Br_2 (Halon-1202), CF_2ClBr (Halon-1211), and CF_2BrCF_2Br (Halon-2402), photolysis from wavelengths >286 nm (which are effective in the troposphere) also contributes to their atmospheric removal.
- For hydrogen containing molecules (CH_3CCl_3, CH_3Cl, CH_3Br, HCFCs, and HFCs), loss due to the OH reaction in the troposphere is dominant (>90%).
- There are a number of new findings since the publication of the JPL-10-6 kinetic data evaluation (Sander *et al.,* 2011):
  - New experimental data are evaluated for CF_3CF_2Cl (CFC-115), NF_3, CF_2Br_2 (Halon-1202), CF_2ClBr (Halon-1211), and CF_2BrCF_2Br (Halon-2402) and used to compute lifetimes in the two-dimensional (2-D) model.
  - Lyman-α absorption cross-section recommendations, which have not been considered in previous evaluations, are provided and uncertainties estimated. Lyman-α photolysis is shown to be a dominant mesospheric loss process, but makes only a minor contribution to the global lifetime.
  - To correct errors in previously reported values, the ultraviolet (UV) absorption cross-section parameterizations for use in model calculations for $CFCl_3$ (CFC-11), CF_2Cl_2 (CFC-12), $CFCl_2CF_2Cl$ (CFC-113), CF_2ClCF_2Cl (CFC-114), $CHClF_2$ (HCFC-22), CH_3CCl_3, CH_3Cl, and CH_3Br are revised. The impacts on the computed lifetime are small, ~ a few percent.
  - The estimated uncertainty in the hydroxyl radical (OH), electronically excited atomic oxygen ($O(^1D)$), and atomic chlorine (Cl) reaction rate coefficients given in this report are, in general, less than those given in the JPL10-6 (Sander *et al.,* 2011) and the IUPAC (Atkinson *et al.*, 2008) data evaluations.
- All the 3-D models used kinetics from *Sanders et al.* (2011) to calculate the lifetimes in this study. In addition, a 2-D model was used to calculate lifetimes and uncertainties using the new kinetic data and evaluate the differences between these kinetic data. The (2-σ) range in calculated atmospheric lifetime due solely to uncertainty in the kinetic and photochemical data of the source gas (at the 2 σ limit) is expressed as a percentage of the value calculated using the recommended values. The lifetime uncertainties range from a low of 6% to as high as 40% (see Table 9 in Chapter 3).
- The contribution of the uncertainties in the molecular oxygen (O_2) absorption cross sections in the Schumann-Runge bands and Herzberg continuum (which were not evaluated in this report) to the model calculated uncertainties in the lifetimes of species primarily removed in the stratosphere (SR) was quantified. The 2σ uncertainties in calculated lifetimes due to uncertainty in O_2 cross sections are estimated to be 15% and 9% for CFC-11 and CFC-12, respectively; the lifetime uncertainty due to uncertainty in the ozone (O_3) cross sections is small (<0.5%) for CFC-11 and CFC-12.

With respect to observation-based methods used to determine lifetimes (see Chapter 4 and Section 6.2 for further descriptions)

- Global atmospheric lifetimes for CFC-11, CFC-12, CFC-113, and CH_3CCl_3 were determined using an inverse modeling method for the period from the late 1990's to the

present. In addition, the model was used in the forward mode to derive steady-state lifetimes using the retrieved parameters. For CFC-11, CFC-12, and CH_3CCl_3 the global lifetimes derived using observations from this time period is within 1% of its respective steady-state lifetime. For CFC-113, the difference is less than 5%.

- Mean regional tropospheric OH abundances were inferred using CH_3CCl_3 observations in a Bayesian inversion using a 12-box model. A modeling exercise confirmed that the 12-box model successfully retrieves the appropriate OH values from three-dimensional (3-D) model simulated time series of surface concentrations for a flux boundary condition tracer simulation. This provides confidence that the OH values inferred from CH_3CCl_3 can be used in the forward model to compute the steady-state lifetimes of the hydrochlorofluorocarbons (HCFCs) and hydrofluorocarbons (HFCs) in Table 1.1.
- Modeled photochemical loss has been combined with observed global distributions of CFC-11, CFC-12 and N_2O in the stratosphere and surface concentrations to calculate the global atmospheric lifetimes (satellite hybrid model). Adjustments were made to estimate the steady-state lifetimes.
- Tracer-tracer correlations have been used to obtain steady-state stratospheric (partial) lifetimes for CFC-12, CFC-113, CCl_4, H-1301, and N_2O relative to CFC-11. This method requires the stratospheric lifetime of CFC-11 as input. The tracer-tracer method was also used to determine the stratospheric lifetimes for CH_3CCl_3, CH_3Cl, H-1211, H-1301, HCFC-22, HCFC-141b, and HCFC-142b. However, those values were not used in deriving the steady state lifetimes for those species in this report.

With respect to model simulated results (see Chapters 3 and 5)

- Lifetimes (global atmospheric and steady-state) were calculated using seven global models (six 3-D CCMs and one 2-D model) using the same standard photochemical data (JPL-10-6).
- Most models perform well on most of the photochemical, kinetic, and transport diagnostics. No overall disqualifying implementation errors were identified in any of the models. However, some specific results from individual models were excluded because of implementation errors.
- Model results from Chapter 5 show that the steady-state lifetime can be approximated by the global atmospheric lifetime during the period when emissions are decreasing.
- Species that are predominantly removed by OH show a large range of lifetimes between models. However, for many models the lifetimes show good straight-line correlations with the simple metrics of global mean tropospheric OH or the lifetime of a reference species such as CH_3CCl_3.
- Species that are destroyed in the stratosphere show a range of model-calculated lifetimes. The lifetimes show a clear correlation with the simulated tropical mean age profile, which depends on the Brewer-Dobson circulation. In particular, the tropical ascent rate through the altitudes of large loss is critical to the calculated lifetimes with faster ascent rates producing shorter lifetimes. The uncertainty (variance) of the 7-model mean lifetime is smaller than the uncertainty due to photochemistry and $\sigma(O_2)$ discussed in Chapter 3.
- It is not clear how the lifetimes of SR (primarily stratospheric removal) species will change by 2100. Some, but not all models, indicate a faster Brewer-Dobson circulation in 2100 and a younger age-of-air. However, for other models the circulation change is not so clear. A thicker (recovered) ozone layer in 2100 leads to reduced photolysis. These two processes lead to cancelling effects on lifetimes in the models. Finally, the change in lifetime will depend on the assumed emission scenarios for the greenhouse gases.

- For a 2100 atmosphere the majority of models indicate a decrease in TR (primarily tropospheric removal) species lifetime due to the combined impact of increasing OH and increasing air temperature.

6.2 What Methods Were Used to Determine Values for Steady-State Lifetimes?

Five methods were used to derive lifetimes (global atmospheric lifetime (GAL) and steady-state lifetime). This section focuses on the four methods which derived steady-state lifetimes using observed concentrations of species in the atmosphere. On the other hand, results from model simulations reported in Chapters 3 and 5 provide values for the modeling method. The modeling method requires photochemical data as input. While no observation is used directly in deriving the model lifetimes, one should not overlook the fact that observations of many species were used to guide the development and provide validation for the models. Chemistry and Transport Models (2-D and 3-D), have improved tremendously since the 1994 lifetimes assessment (Kaye *et al.,* 1994). Some of the models have evolved into comprehensive atmospheric chemistry climate models that provide a self-consistent framework for calculating lifetimes. However, their accuracy depends on their ability to realistically represent important atmospheric processes involving chemistry, transport, and radiation. Errors in loss rates or in the transport time through the altitude range where loss is important will lead to biases in model calculated lifetimes. Model lifetimes in this report are calculated for a particular climate (e.g., present day composition and meteorology) based on the current global budgets, with corrections for being out of steady state. In the modeling studies, the focus has been on lifetime as defined by photochemical reactions occurring in the atmosphere. Effects on removal by deposition (to land or ocean) are added afterward as a partial lifetime.

The steady-state global lifetime is not a directly observable quantity. However, observed concentrations of a species in the atmosphere can be used to determine lifetimes with the help of a model. Lifetimes derived from this combined method have greatly improved with the availability of global, satellite-based retrievals of gas concentrations. Because the measured concentrations are influenced by actual emission histories and the state of the atmosphere at the time of the measurements, they can only provide information on the global atmospheric lifetime at the measurement time. Nevertheless, these values can be adjusted to obtain estimates for the steady-state lifetime. For species with available observations, four methods were used to derive lifetimes:

(1) Inverse modeling (Section 4.3.1) uses a 12-box model to retrieve the global atmospheric lifetime from the time series of observed burden (derived from surface concentrations) and the emissions. This method does not require detailed knowledge of the chemical properties of the molecule, but the information is useful for choosing an a priori value in the inversion process, and in relating burden to surface concentration. The retrieved lifetime values can be used in the same 12-box model in the forward mode to compute steady-state lifetimes. This method was used to derive lifetimes for CFC-11, CFC-12, CFC-113, and CH_3CCl_3.
(2) A satellite hybrid method (Section 4.3.4) uses vertically resolved concentrations of the species in the stratosphere and photolysis model-derived loss rates to derive global lifetimes. This method is most useful for SR species. The calculated values can be adjusted to approximate the steady-state lifetimes. This method is used in this report to derive lifetimes for CFC-11, CFC-12, and N_2O.

(3) The tracer-tracer correlation method (Section 4.4) uses simultaneously observed concentrations of a pair of species in the stratosphere (either in situ or satellite) to determine relative stratospheric lifetimes. Data are available for CFC-11, CFC-12, CFC-113, CCl_4, N_2O, H-1211, H-1301, CH_3CCl_3, CH_3Cl, CH_4, HCFC-22, HCFC-141b, and HCFC-142b. A stratospheric lifetime for CFC-11 is required to estimate the absolute lifetimes.

(4) The proxy tropospheric OH concentration is a by-product of the inverse modeling retrieval when applied to CH_3CCl_3 (Section 4.3.1.4). The partial lifetime due to OH loss in the troposphere for other hydrogen-containing species (e.g., HCFCs and HFCs) is computed using the 12-Box forward model. The method is equivalent to the scaling using the reaction rate constant with OH (Spivakovsky *et al.,* 2000). The partial lifetime is then combined with other information to obtain steady-state lifetimes.

Figure 6.1 explains the flow of information on how the lifetime values from the five methods are combined to provide a single recommended value. The best estimate and the associated uncertainty from each method are provided in the relevant chapter. We treat the value from each method as an estimator of the recommended steady-state lifetime. The best estimate from a method is often the mean of several individual estimates obtained using different data or tools. For example, simulated lifetime values from different models are considered to be individual estimates, and the mean value is identified as the best estimate. For observation-based methods, individual estimates arise when different data sets are used to derive the lifetime. Through analyses of the methodology and by propagating the uncertainties of the input data, we derive an associated uncertainty estimate for each method. The best estimates from each method (the estimators) are then combined using a weighted average to produce the recommended lifetime. We provide two ranges for the recommended lifetime uncertainties (both are 2σ). The first range, defined by Equation (6.11) in the Appendix, is the weighted mean of the variances from each method taking into account the covariance between estimators. This provides the range for the most likely values. The second, defined by Equation (6.6) in the Appendix, corresponds to the joint distribution of the individual variances around the arithmetic (i.e., unweighted) mean of the estimators. This represents the full range of the lifetime value estimates. The interpretation is that values outside of this second range are unlikely to be supported by future evaluations. Details of the uncertainty derivations are provided in the Appendix.

6.3 What Are the Recommended Steady-State Lifetimes and Uncertainties?

The recommended steady-state lifetimes are presented in three tables, grouped essentially by the methods used for determining the steady-state lifetimes. The species in Table 6.1 include most of the stratospheric removal (SR) species. For some species, data are available for several observation-based methods. Species in Table 6.2 are all tropospheric (primarily OH) removal species (TR). As will be discussed below, the lifetimes in this group are determined using the 12-box forward model. Table 6.3 provides results for three Halons and NF_3. These lifetimes are from the 2-D model calculated using new photochemical data from this report. All mean lifetimes and uncertainties are calculated by averaging the inverse of lifetime (i.e., loss rates). The uncertainty range is calculated formally using the methodology described in the Appendix. The column LOSU (Level of Scientific Understanding) is an expert judgment of the reliability of the recommended value, taking into account the number of estimators, and the ability of the estimator(s) to provide good estimates for the steady-state lifetimes.

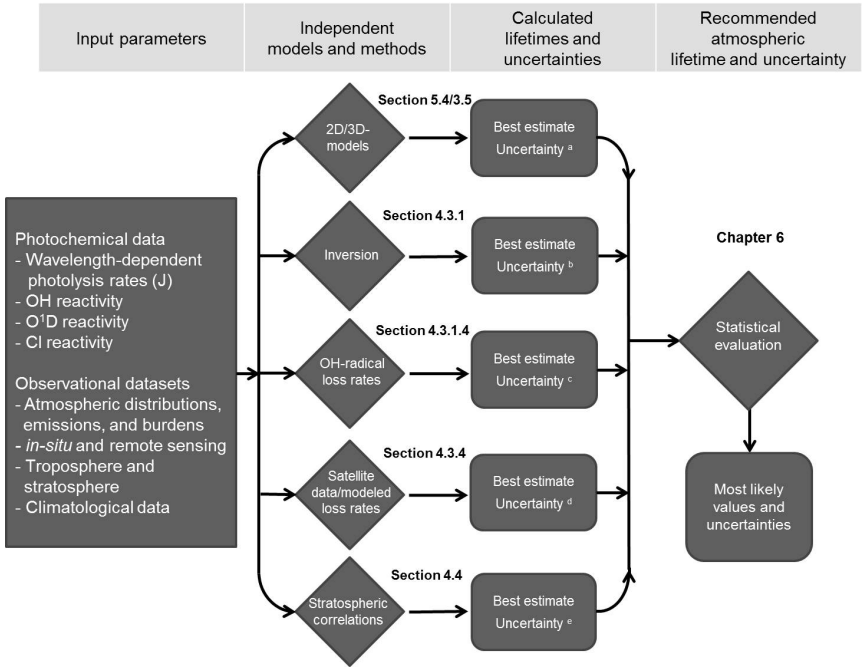

Figure 6.1. Information flow chart for producing recommended steady-state atmospheric lifetime values and uncertainties.

[a] **2-D/3-D models:** Best estimate: Model averages; Uncertainty: model variance + uncertainty from kinetic data.
[b] **Inversion:** Best estimate: Average based on independent retrievals using NOAA and AGAGE time series; Uncertainty: From retrieval model based on knowledge of emission history, length of time series.
[c] **OH-Radical Loss Rates:** Best estimate: from 12-box forward model + 2-D model stratospheric partial lifetime; Uncertainty: from uncertainties in retrieved tropospheric OH concentration and uncertainty in k-OH.
[d] **Satellite data/modeled loss rates:** Best estimate: average from several satellite data sets; Uncertainty: estimated from uncertainties in concentrations and kinetic data.
[e] **Stratospheric correlations (tracer-tracer):** Best estimate: weighted average from different data sets made at different location and time; Uncertainty: standard deviation, and uncertainty in the assumed CFC-11 stratospheric lifetime (as determined from the other methods).
Details of the methods are explained in the respective chapters. All averaging is done using the inverse of lifetime (i.e., loss rates).

Figure 6.2 graphically summarizes the steady-state lifetime estimates determined for the 27 species listed in Table 1.1, including estimates of the uncertainty distribution. Only CFC-11, CFC-12, CFC-113, and N_2O have sufficient observations to allow lifetimes to be determined using three or four methods. We treat the value from each method as an estimator of the steady-state lifetime. The recommended estimates of the lifetime (shown by the black vertical bars in Figure 6.2) correspond to the weighted-mean of the different estimators. Each method has an associated estimate of the variance or uncertainty. For readability, we have combined the observation-based estimated values into one single distribution as explained in the Appendix.

Four species in Table 6.1 (CFC-11, CFC-12, CFC-13, and N_2O) have more than two observation-based estimators for determining the recommended steady-state lifetime. Three of the four are designated as having high LOSU in the recommended value. In general, the

inversion method has the smallest estimated uncertainties. This is a result of the long data record, and the fact that their emissions have been close to zero over the past decade. The satellite methods have larger uncertainties. For CFC-11, the available satellite data simply do not have fine enough resolution to resolve the vertical gradient in the lower stratosphere. In calculating the weighted average for CFC-11, the satellite method was assigned a 0.17 weighting (as opposed to 1/3) as one of the three estimators. Finally, the estimated uncertainties associated with the model derived lifetimes are smaller than those associated with the other estimators. These model weightings are 0.47 for CFC-11, 0.40 for CFC-113, and 0.44 for N_2O (as opposed to 1/3); and 0.33 for CFC-12 (as opposed to ¼).

We included (up to) three covariance terms in computing the most likely values for the six source gases in Table 6.1. These covariances are found between:

- The model and the satellite estimators arising from the uncertainty in the chemical data for the source gas, and from the uncertainty in the O_2 cross-section.
- The tracer-tracer and model estimators arising from the uncertainty in the O_2 cross section and the uncertainty in model transport. Both these uncertainties similarly affect the model-derived lifetimes of the source gas and of CFC-11, the latter of which is needed to determine the lifetime of the source gas from the tracer-tracer method.
- The tracer-tracer and the satellite estimators arising from the uncertainty in the O_2 cross-section.

All of the covariance terms are positive and increase the range of the most likely values. Our results suggest that a reduction in the uncertainty in the O_2 cross-section will reduce the range for the most likely values for the six source gases.

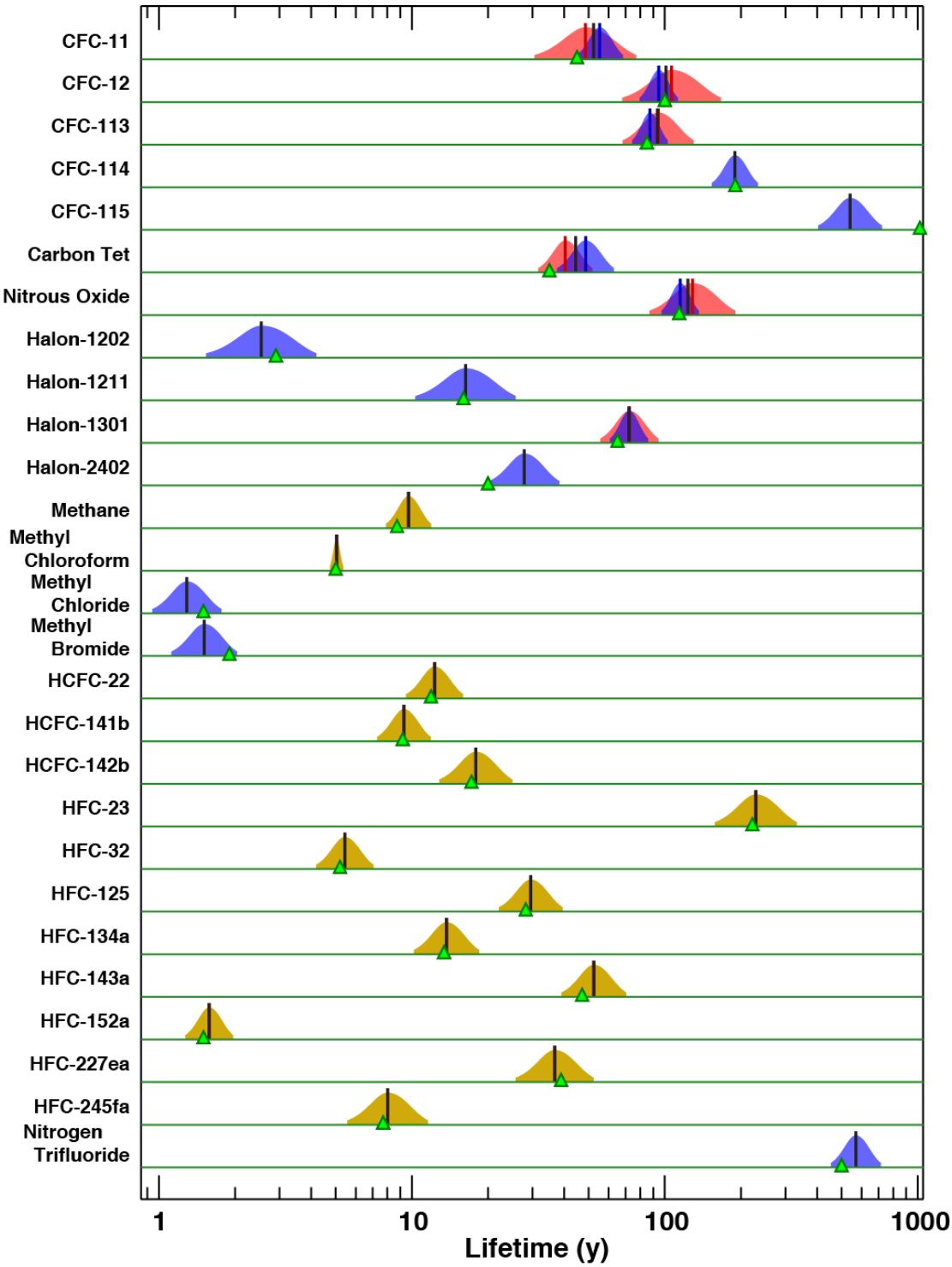

Figure 6.2. Recommended steady-state lifetime estimates (vertical black lines), lifetime estimates from models (blue) and observations (red) for the species in Table 1.1. The estimated uncertainties from models (light blue) and observations (light red) are also shown. The uncertainty estimates for the HCFCs and HFCs (shown in green) are from the uncertainty in the retrieved OH concentration and uncertainties in the reaction rate constants. Lifetime estimates from previous reports (WMO, 2011; IPCC, 2007) are indicated by the green triangles.

Table 6.1. Recommended estimates for steady-state lifetimes of stratospheric removal species. Values are for steady-state lifetime due to photochemical removal in the atmosphere. See text for discussion of the "most likely values", the "possible range". The weighting factors for the estimators, defined to be proportional to the inverse of the standard deviation (σ), are included.

Species	WMO (2011)	Observation-Derived Inverse Lifetime						Model-Derived Inverse Lifetime		Recommended Lifetime					Level of Scientific Understanding (LOSU)
		Inversion		Tracer-Tracer*		Satellite.					Possible range				
	τ (Yr)	Weight 1/τ (Yr $^{-1}$)	σ(%)	Weight 1/τ (Yr $^{-1}$)	σ(%)	Weight 1/τ (Yr $^{-1}$)	σ(%)	Weight 1/τ (Yr $^{-1}$)	σ(%)	τ (Yr)		Most likely range			
CFC-11	45	0.36 (53)$^{-1}$	15%			0.17 (45)$^{-1}$	25%	0.47 (55)$^{-1}$	12%	**52**	35	43	67	89	High
CFC-12	100	0.21 (111)$^{-1}$	17%	0.25 (102)$^{-1}$	13%	0.20 (107)$^{-1}$	18%	0.33 (95)$^{-1}$	9%	**102**	78	88	122	151	High
CFC-113	85	0.38 (109)$^{-1}$	11%	0.22 (83)$^{-1}$	15%			0.40 (87)$^{-1}$	9%	**93**	69	82	109	138	Medium Same method as CFC-11 and CFC-12, but shorter data record
CCl_4 [a]	35			0.47 (40)$^{-1}$	14%			0.53 (49)$^{-1}$	15%	**44**	33	36	58	67	Medium Fewer estimators than CFC-11 and CFC-12
Nitrous Oxide	114			0.33 (144)$^{-1}$	16%	0.23 (116)^{1}	18%	0.44 (115)$^{-1}$	9%	**123**	91	104	152	192	High
Halon-1301	65			0.38 (72)$^{-1}$	15%			0.62 (72)$^{-1}$	9%	**72**	58	61	89	97	Medium Fewer estimators than CFC-11 and CFC-12
CFC-114	190							1.0 (189)$^{-1}$	12%	**189**	153			247	Low No observation-based numbers
CFC-115 [b]	1020							1.0 (540)$^{-1}$	17%	**540**	404			813	Low No observation-based numbers

[a] The lifetime corresponds to the steady-state lifetime due to photochemical removal in the stratosphere. See text for the discussion of total lifetime including ocean and soil sinks.

[b] The model value is from the 2-D model using the photochemical data from this report.

Table 6.2. Recommended estimates for steady-state lifetimes for tropospheric removal species. The quoted possible range corresponds to 2σ uncertainty.

Species	WMO (2011)	Observation-Derived Inverse Lifetime				Model-Derived Inverse Lifetime		Recommended Lifetime			Level of Scientific Understanding (LOSU)
		Inversion		Forward 12-Box Model + Modeled Stratospheric Lifetime							
	τ (Yr)	1/τ (Yr $^{-1}$)	σ(%)	1/τ (Yr $^{-1}$)[1]	σ(%)[a]	1/τ (Yr $^{-1}$)	σ(%)	τ (Yr))	Possible range		
Methyl Chloroform [b]	5.0	$(5.0)^{-1}$	3%	$(5.4)^{-1}$	12%			**5.0**	4.7	5.4	High Based on inversion of CH_3CCl_3, but has to parameterize ocean sink.
HCFC-22	12			$(12)^{-1}$	16%			**12**	9.3	18	Medium Observation constraint based on CH_3CCl_3
HCFC-141b	9.2			$(9.4)^{-1}$	15%			**9.4**	7.2	13.5	
HCFC-142b	17.2			$(18)^{-1}$	14%			**18**	14	25	
HFC-23	222			$(228)^{-1}$	21%			**228**	160	394	
HFC-32	5.2			$(5.4)^{-1}$	17%			**5.4**	4.0	8.2	
HFC-125	28.2			$(31)^{-1}$	18%			**31**	22	48	
HFC-134a	13.4			$(14)^{-1}$	18%			**14**	10	21	
HFC-143a	47.1			$(51)^{-1}$	19%			**51**	38	81	
HFC-152a	1.5			$(1.6)^{-1}$	15%			**1.6**	1.2	2.2	
HFC-227ea	38.9			$(36)^{-1}$	21%			**36**	25	61	
HFC-245fa	7.7			$(7.9)^{-1}$	22%			**7.9**	5.5	14	
Methane [c]	8.7/12			$(9.8)^{-1}$	15%			**9.8**	7.6	14	
Methyl Chloride [d]	1.5					$(1.3)^{-1}$	18%	**1.3**	0.9	2.0	Medium See footnote d
Methyl Bromide [d]	1.9					$(1.5)^{-1}$	17%	**1.5**	1.1	2.3	

[a] The quoted standard deviation accounts for the uncertainties in the retrieved OH, and OH reaction rate constant as derived in Chapter 3.

[b] The number in the WMO column is the total lifetime (including the ocean sink). The value from the inversion method for CH_3CCl_3 also corresponds to the total global atmospheric lifetime. The recommended value is the steady-state lifetime based on the inversion. The steady-state partial lifetime due to photochemical removal in the atmosphere is also provided in the "forward 12-box model" column. When combined with the 94 year lifetime from the ocean sink, this will provide a total lifetime of 5.1 years. This is well within the uncertainty associated with the inversion value.

[c] The 12-year value in the WMO column is the response lifetime. All other values correspond to the steady-state lifetime for CH_4.

[d] The values (including the WMO column) correspond to lifetime due to removal by OH. The values in the table are from model simulations. We could have (but did not) use the forward model in this calculation.

The CFC-11 lifetime is a weighted average of the model estimates, the satellite-hybrid observation method, and the inverse model of observations. The CFC-12 lifetime uses the same techniques but also includes the tracer-tracer observations method. CFC-11 and CFC-12 have recommended lifetimes of 52 and 102 years, respectively. These are not significantly different from the values provided in previous assessments (see Figure 6.3). What is more notable is that while previous assessments provided uncertainty estimates for each estimator, we combine the uncertainties into two ranges. As explained in Section 6.2, these are given as a "most likely" range and a "possible" range. For CFC-11 the possible range is 37 - 92 years (thin red line on RHS of Figure 6.3) while the likely range is 43 - 67 years (thick red line on RHS of Figure 6.3). Similarly, for CFC-12 the possible range is 78 – 149 (thin blue line on RHS of Figure 6.3) while the likely range is 88 - 122 years (thick blue line on RHS of Figure 6.3). As noted above, these possible ranges span the uncertainties of all of the estimated 2σ values. The most likely ranges reflect a reduction in the uncertainty resulting from the overlap of the distributions, and therefore a tighter estimate of the recommended uncertainty. It is clear from Figure 6.3 that these combined ranges are, in most cases, smaller than the individual ranges cited in previous assessments.

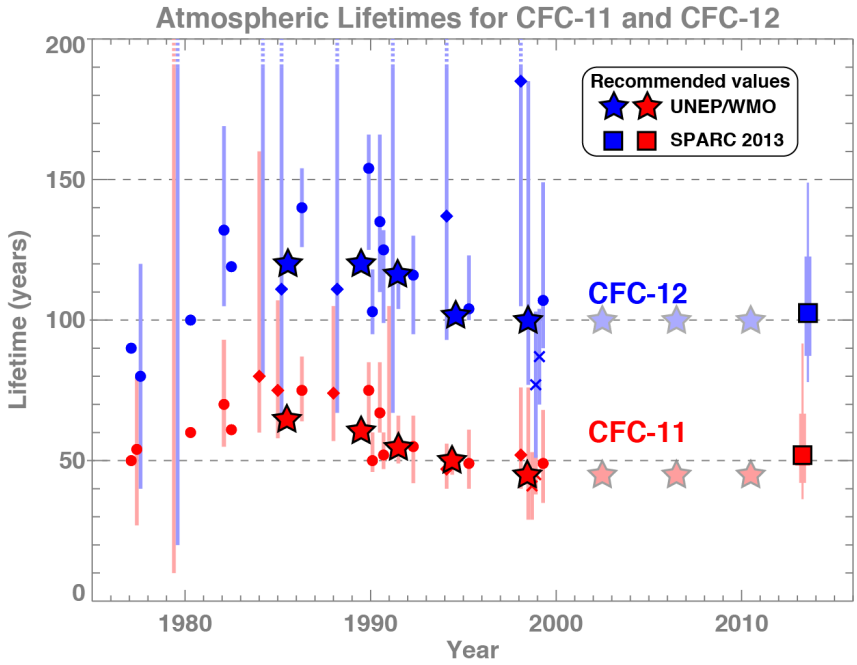

Figure 6.3. Recommended steady-state lifetimes and uncertainty ranges for CFC-11 and CFC-12. Results from previous assessment reports are shown with respect to the year they were published. The recommended values of CFC-11 and CFC-12 from this report are 52 and 102 years, respectively (right hand side). The possible ranges are 37-92 years (thin red) for CFC-11 and 78-149 years (thin blue) for CFC-12. The most likely ranges are 43-67 years (thick red) for CFC-11 and 88-122 years (thick blue) for CFC-12.

For CCl_4 the recommended steady-state lifetime of 44 years is calculated only from the removal by photochemical reactions in the stratosphere (excluding the ocean uptake and soil removal). This is larger than the 35 years from recent WMO reports. Previously, the 35 year lifetime was combined with an oceanic removal lifetime of 94 years to obtain a total lifetime of 26 years. That lifetime was found to be too short to reconcile the observed tropospheric trends with estimated emissions. The current estimate for the oceanic lifetime is 81 years,

with a soil removal lifetime of 195 years (see Chapter 4). The combined lifetime is 25 years. Thus, the issue for the CCl_4 budget, as discussed in Montzka and Reimann (2011), remains.

Values in Table 6.2 were generated using the 12-box model described in Section 4.3.1. An inversion exercise was first performed using the time series of the observed surface concentration for CH_3CCl_3. The 12-box model retrieval gives a total global atmospheric lifetime of 5.0 years for CH_3CCl_3. The uncertainty is 3%, giving a 2-σ range of 4.7 – 5.3 years. In the inversion, an ocean sink corresponding to a partial lifetime of 83 years was assumed along with in situ photochemical removal in each of the 12-boxes. The retrieved removal rate in the troposphere can be converted to an average OH concentration in each box. It is estimated that the uncertainty for the average OH concentration is 12%. This includes the uncertainty associated with assigning the ocean partial lifetime for CH_3CCl_3, and the uncertainty in the reaction rate constant of CH_3CCl_3 with OH.

The averaged OH values were then used in the forward model to compute the partial steady-state lifetime due to reaction with OH in the troposphere for the rest of the species listed in Table 6.2. The tropospheric partial lifetime was combined with the partial stratospheric lifetime (appropriately defined to coincide with the stratosphere in the 12-box model) from the 2-D model to provide a total lifetime. The uncertainty range is based on the uncertainty in the average OH concentration, the uncertainty in the reaction constant with OH, and the uncertainty in the partial stratospheric lifetime.

The 3-D models use JPL-10-6 photochemical data in their simulations. There were significant revisions in the data for the 4 species listed in Table 6.3 based on the work in Chapter 3. As a result, we base the lifetime recommendation on the 2-D model results which used this new kinetic data.

Table 6.3. Model-calculated values for steady-state lifetimes. The values are from the 2-D model using the kinetic data from this report. The quoted possible range corresponds to 2σ uncertainty.

Species	WMO (2011)	Model derived Inverse Lifetime		Recommended Lifetime			Level of Scientific Understanding (LOSU)
	τ (Yr)	1/τ (Yr^{-1})	σ(%)	τ (Yr)	Possible range		
Halon-1202	2.9	$(2.5)^{-1}$	33%	**2.5**	1.5	7.3	Low
Halon-1211	16	$(16)^{-1}$	29%	**16**	10	39	Low
Halon-2402	20	$(28)^{-1}$	19%	**28**	20	45	Low
NF_3	500	$(569)^{-1}$	13%	**569**	454	764	Low

6.4 What Can Be Done in Future Studies to Reduce the Uncertainties?

This report documents the use of advances in photochemical data and chemistry climate modeling, along with an abundance of high quality observations, to improve estimates of lifetimes and their uncertainties for many ODSs and related species. For some species, uncertainties remain large due to limited observations or uncertainties related to loss processes. Further improvements to lifetime estimates may be obtained with gains in knowledge in two areas: first, the scientific understanding of the processes influencing lifetimes and applying the new understanding to analyses of existing data; and second, more (different locations and times) accurate measurements to constrain budgets.

The photolysis rate of a species depends on the absorption cross-section of the species and the availability of photons. In a photolysis calculation, the latter depends on the parameterization of the O_2 cross sections in the Schumann-Runge Bands. While no attempt was made in this report to examine atmospheric opacity, it is noted as an important uncertainty (up to 15% (2-σ uncertainty) for CFC-11). Measurements of short-wave actinic fluxes in the tropical stratosphere could help to better constrain CFC loss rates. Finally, the temperature dependence of the absorption spectra of CFC-11 and CFC-12 has been identified in this report as major sources of uncertainty.

Important questions have emerged on the limitation of the theoretical understanding of the impact of inter-annual variability and the long-term trends of stratospheric circulation on quantities relevant for lifetime estimates. This suggests that some of the differences between lifetime estimates based on observations in different years could be real, rather than reflecting inaccuracies in different estimates. Another source of uncertainty is the variability of lifetime estimates due to the interannual variability in stratospheric transport caused by the quasi-biennial oscillation (QBO) (e.g., Tian *et al.,* 2006; Punge *et al.,* 2009).

There is scientific debate regarding the theoretical basis for using tracer-age correlations to estimate absolute lifetimes. The lifetimes of stratospheric removal (SR) species depend critically on atmospheric transport in the lower-mid stratosphere, in particular ascent rates in the tropics and recirculation mixing rates from mid-latitudes into the tropics. Numerous diagnostics exist for testing model transport in this region (SPARC, 2010; Strahan *et al.,* 2011), but their usefulness depends on the quality and coverage of observations. Improved observational constraints on tropical transport processes could be provided with wider coverage of tracers that diagnose age-of-air or age spectrum (e.g., CO_2 and N_2O) and the tropical 'tape recorder' (e.g., H_2O and CO). The interpretation of the observations, however, may depend strongly on an improved understanding of how the QBO and interannual variability affect stratospheric transport, and consequently lifetimes.

Surface flux boundary conditions (FBCs) for tracers allow chemistry and transport to evolve in a self-consistent manner within a model. Their use in CCM simulations would remove the artificial constraint imposed by specifying mixing ratio boundary conditions (MBCs) from a pre-computed scenario. However, the database for emission and surface sink estimates is not sufficient to allow all tracers discussed in this report to be treated in this way. Where sufficient data exist models should use FBCs, especially for species that have a large trend in atmospheric burden. For species with poorly constrained atmospheric emissions and/or surface sinks, or a fairly constant atmospheric burden, MBCs are still preferable.

Chapter 4 concludes that accurate and highly vertically resolved CFC profiles are essential for the techniques deducing CFC lifetimes from observations. For the satellite hybrid method (Minschwaner *et al.,* 2013), accurate, high vertical resolution profiles in the tropics are most important. For the tracer/tracer correlation methods, accurate information is needed on tracer slopes in the lower extratropical stratosphere, close to the tropopause. Here, improved retrievals of previously analysed data sets (e.g., MIPAS) and the extension of the analysis to additional data sets (e.g., HIRDLS) may lead to more accurate vertical profiles. However, the vertical resolution of the satellite data results is a fundamental limitation on the possible degree of the uncertainty reduction. *In situ* observations in the lower stratosphere will help to constrain this fundamental limitation of the satellite data when used for the satellite hybrid method and the tracer/tracer method.

It is essential to continue and extend ground-based measurement networks. Further, solidly vetted emission data sets for all the compounds evaluated herein and a better characterization of non-atmospheric (e.g., oceanic) sinks of these compounds is important for both inverse and forward model studies for some of the compounds.

The lifetimes of tropospheric removal (TR) species depend overwhelmingly on the abundance of tropospheric OH. Using direct observations to constrain the highly variable local OH concentration is problematic, although an observation-inferred global mean OH abundance has been derived in this report. Additional observational constraints on OH are needed, especially the mean abundance in the tropical lower troposphere where a large fraction of TR species' destruction occurs. Modelled tropospheric mean OH values vary considerably. Model-model intercomparisons are needed to understand the cause of these differences. While there are a number of surface stations measuring TR species, there are few measurements of their vertical and latitudinal distributions. Observations of a range of species with primarily OH loss would constrain both model estimate of losses and transport pathways.

The 44-year steady-state atmospheric lifetime of CCl_4 determined in this report is substantially longer than the 35 years from WMO (2011). However, the estimate of the partial lifetime for the oceanic sink has decreased from 93 years to 81 years (Section 4.3.3.2). Assuming a 195-year partial lifetime for the soil sink (Montzka and Reimann *et al.,* 2011), this yields a total global lifetime of 25 years, comparable to the 26 years from WMO (2011). This confirms the imbalance between sinks and sources as elaborated therein. However, the value for the soil sink is only based on a few campaigns in specific ecosystems and the value for the oceanic sink comes from a single study (Yvon-Lewis and Butler, 2002). Therefore, the new total lifetime of 25 years should only be used in a qualitative way for assessing the global sources until soil and oceanic sink terms are better constrained.

6.5 References

Atkinson, R., D. L. Baulch, R. A. Cox, J. N. Crowley, R. F. Hampson, R. G. Hynes, M. E. Jenkin, M. J. Rossi, J. Troe, and T. J. Wallington, Evaluated kinetic and photochemical data for atmospheric chemistry: Volume IV - gas phase reactions of organic halogen species, *Atmos. Chem. Phys.*, *8*, 4141-4496, 2008.

IPCC, Climate Change 2007: The Physical Science Basis. Contribution of Working Group I to the Fourth Assessment Report of the Intergovernmental Panel on Climate Change (S. Solomon, D. Qin, M. Manning, Z. Chen, M. Marquis, K. B. Averyt, M. Tignor, and H. L. Miller (eds.), Cambridge University Press, Cambridge, United Kingdom, and New York, NY, USA, 996 pp., 2007.

Kaye, J. A., S. A. Penkett, and F. M. Ormond (eds.), *Report on Concentrations, Lifetimes, and Trends of CFCs, Halons, and Related Species*, NASA Reference Publication 1339, Washington, D.C., 1994.

Minschwaner, K., L. Hoffmann, A. Brown, M. Riese, R. Müller, and P. B. Bernath, Stratospheric loss and atmospheric lifetimes of CFC-11 and CFC-12 derived from satellite observations, *Atmos. Chem. Phys., 13,* 4253-4263, 2013.

Montzka, S. A., and S. Reimann (Coordinating Lead Authors), A. Engel, K. Krüger, S. O'Doherty, and W. T. Sturges (Lead Authors), Ozone-Depleting Substances (ODSs) and Related Chemicals, Chapter 1 in *Scientific Assessment of Ozone Depletion: 2010, Global Ozone Research and Monitoring Project–Report No. 52*, 516 pp., World Meteorological Organization, Geneva, Switzerland, 2011.

Punge, H. J., P. Konopka, M. A. Giorgetta, and R. Müller, Effects of the quasi-biennial oscillation on low-latitude transport in the stratosphere derived from trajectory calculations, *J. Geophys. Res.*, *114*, D03102, doi: 10.1029/2008JD010518, 2009.

Sander, S. P., J. Abbatt, J. R. Barker, J. B. Burkholder, R. R. Friedl, D. M. Golden, R. E. Huie, C. E. Kolb, M. J. Kurylo, G. K. Moortgat, V. L. Orkin, and P. H. Wine, *Chemical Kinetics and Photochemical Data for Use in Atmospheric Studies, Evaluation Number 17,* JPL Publication 10-6, Jet Propulsion Laboratory, California Institute of Technology 2011.

SPARC CCMVal (Stratospheric Processes And their Role in Climate), *SPARC CCMVal Report on the Evaluation of Chemistry-Climate Models*, edited by V. Eyring, T. G. Shepherd, and D. W. Waugh, SPARC Report No. 5, WCRP-132, WMO/TD-No. 1526, http://www.atmosp.physics.utoronto.ca/SPARC/ccmval_final/index.php, 2010.

Spivakovsky, C. M., J. A. Logan, S. A. Montzka, Y. J. Balkanski, M. Foreman-Fowler, D. B. J. Jones, L. W. Horowitz, A. C. Fusco, C. A. M. Brenninkmeijer, M. J. Prather, S. C. Wofsy, and M. B. McElroy, Three-dimensional climatological distribution of tropospheric OH: Update and evaluation, *J. Geophys. Res.*, *105* (D7), 8931-8980, doi: 10.1029/1999JD901006, 2000.

Strahan, S. E., A. R. Douglass, R. S. Stolarski, H. Akiyoshi, S. Bekki, P. Braesicke, N. Butchart, M. P. Chipperfield, D. Cugnet, S. Dhomse, S. M. Frith, A. Gettelman, S. C. Hardiman, D. E. Kinnison, J.-F. Lamarque, E. Mancini, M. Marchand, M. Michou, O. Morgenstern, T. Nakamura, D. Olivié, S. Pawson, G. Pitari, D. A. Plummer, J. A. Pyle, J. F. Scinocca, T. G. Shepherd, K. Shibata, D. Smale, H. Teyssèdre, W. Tian, and Y. Yamashita, Using transport diagnostics to understand chemistry climate model ozone simulations, *J. Geophys. Res., 116,* D17302, doi: 10.1029/2010JD015360, 2011.

Tian, W., M. P. Chipperfield, L. J. Gray, and J. M. Zawodny, Quasi-biennial oscillation and tracer distributions in a coupled chemistry-climate model, *J. Geophys. Res.*, *111*, D20301, doi: 10.1029/2005JD006871, 2006.

WMO (World Meteorological Organization), *Scientific Assessment of Ozone Depletion: 2010, Global Ozone Research and Monitoring Project–Report No. 52*, Geneva, Switzerland, 2011.

Yvon-Lewis, S. A., and J. H. Butler, Effect of oceanic uptake on atmospheric lifetimes of selected trace gases. *J. Geophys. Res.*, *107* (D20), 4414, doi: 10.1029/2001JD001267, 2002.

Appendix: Estimating Uncertainties of Joint and Sampling Distributions

Each lifetime measurement (or estimate or observation) is described by a true value and an uncertainty (following standard statistical methods, e.g., Wilks, 1995). We express this mathematically as:

$$x_{ai} = A_a + \varepsilon_{ai} \tag{6.1}$$

The x denotes the measurement, the a subscript denotes the a^{th} "technique" (e.g., a satellite observation, model observation, inversion, etc.), the i subscript denotes that this is the i^{th} observation (assuming we can repeat the observation multiple times), A denotes the true value that we are trying to measure, and ε_{ai} is the error of the observation that is random and normally distributed. The mean ($\bar{x}_a$) and variance (S_a)are conventionally estimated as:

$$\bar{x}_a = \frac{\sum_{i=1}^{n} x_{ai}}{n}, S_a^2 = \frac{\sum_{i=1}^{n} (x_{ai} - \bar{x}_a)^2}{n-1} \tag{6.2}$$

The Joint Distribution

We first consider combining values from three techniques into a joint distribution (hereafter abbreviated as the J-distribution):

$$\begin{aligned} x &= [x_{a1}, x_{a2}, x_{a3}, ..., x_{b1}, x_{b2}, x_{b3}, ..., x_{c1}, x_{c2}, x_{c3}, ...] \\ &= [A_a + \varepsilon_{a1}, A_a + \varepsilon_{a2}, A_a + \varepsilon_{a3}, ... \\ &\quad A_b + \varepsilon_{b1}, A_b + \varepsilon_{b2}, A_b + \varepsilon_{b3}, ... \\ &\quad A_c + \varepsilon_{c1}, A_c + \varepsilon_{c2}, A_c + \varepsilon_{c3}, ...] \end{aligned} \tag{6.3}$$

Here the a subscript denotes the first technique for estimating a lifetime, while the b and c subscripts denotes the second and third techniques. There are n_a, n_b , and n_c observations in the three observation distributions respectively. The mean ($\bar{x}_J$) and variance (S_J^2) of this J-distribution (denoted by the J subscript) are written:

$$\bar{x}_J = \frac{n_a \bar{x}_a + n_b \bar{x}_b + n_c \bar{x}_c}{n_a + n_b + n_c} \tag{6.4}$$

$$S_J^2 = \frac{(n_a - 1)S_a^2 + (n_b - 1)S_b^2 + (n_c - 1)S_c^2 + n_a(\bar{x}_a^2 - \bar{x}_J^2) + n_b(\bar{x}_b^2 - \bar{x}_J^2) + n_c(\bar{x}_c^2 - \bar{x}_J^2)}{(n_a + n_b + n_c - 1)} \tag{6.5}$$

The J-distribution's S_J quantifies the full range of our lifetime value estimates. In this formulation, there are a total of n_a+n_b +n_c observations in the J-distribution. If we assume that $n_a = n_b = n_c = n$, and that $n>>1$, then we can simplify Equations (6.4) and (6.5) to:

$$\bar{x}_J = \frac{\bar{x}_a + \bar{x}_b + \bar{x}_c}{3}, S_J^2 = \frac{S_a^2 + S_b^2 + S_c^2 + \bar{x}_a^2 + \bar{x}_b^2 + \bar{x}_c^2 - 3\bar{x}_J^2}{3} \tag{6.6}$$

This expression shows that S_J^2 is a function of both the individual variances of the separate distributions, and of the differences of the means from $\bar{x}_J$.

As a simple example of the J-distribution (Figure 6.A1), we will assume three normally distributed functions with means and one standard deviations of: (a) 55.3±6.5 (red), (b) 53.0±7.8 (blue), and (c) 44.7±11.4 (green). In this example, we use the lifetime values directly, but note that the actual calculations in Chapter 6 are performed using loss frequencies (i.e., the inverse of the lifetime, e.g., 1/55.3, 1/53.0, and 1/44.7). Using a normal distribution random number generator, we generate a large number of values to represent each distribution and then "estimate" the individual means and variances ($\bar{x}_a, \bar{x}_b, \bar{x}_c, S_a^2, S_b^2$, and S_c^2.) according to Equation (6.2). As expected, these values correspond to the mean values and standard deviations that were assigned. Similarly, we combine all of these values according to (6.3) and estimate the mean and standard deviations, again using Equation (6.2) to obtain $\bar{x}_J$ and S_J^2. The J-distribution is shown in Figure 6.A1 as the black curve.

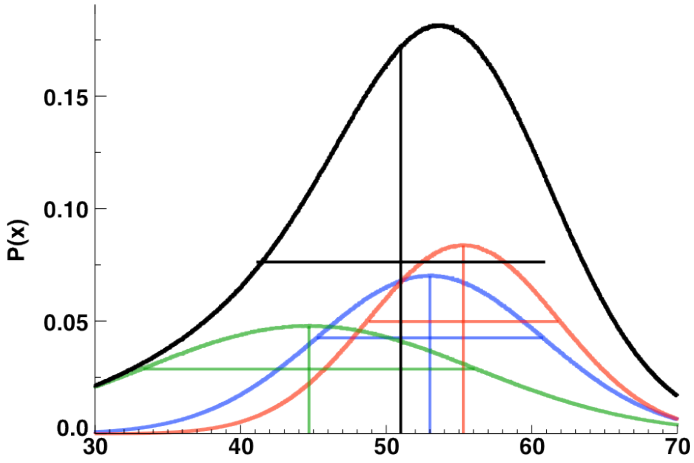

Figure 6.A1. Three normal distributions representing the results from measurements made using three difference methods are combined to form the Joint-distribution (J-distribution). The probability distribution functions of the three populations (red, blue, and green) with different means (vertical lines) and standard deviations (horizontal lines) as shown. The J-distribution is shown in black. The magnitudes of the red, blue, and green distributions have been decreased by 1/3 to show how they sum to the black curve.

The direct estimate of the mean from this J-distribution is 51 with a standard deviation of 9.9, determined from (6.2). These direct estimates are in near exact agreement with the values derived from the individual distribution estimates using (6.6). The mean value in Figure 6.A1 is shown by the vertical black line, while the horizontal black bar shows the ±1σ values (square root of the variance estimate S_J^2) about the mean. As is clear from the figure, this variance describes the range of all of the values. Note that this distribution is not normally distributed.

The Sampling Distribution

An alternative to the J-distribution is to sample from each technique and then perform a weighted average of those samples together. We will refer to this as the sampling distribution of the weighted mean (hereafter, the SWM-distribution). We can describe this technique mathematically assuming three observational techniques according to:

$$\begin{aligned} x &= [w_a x_{a1} + w_b x_{b1} + w_c x_{c1},\ \ w_a x_{a2} + w_b x_{b2} + w_c x_{c2},\ w_a x_{a3} + w_b x_{b3} + w_c x_{c3},\ ...] \\ &= [w_a A_a + w_b A_b + w_c A_c + w_a \varepsilon_{a1} + w_b \varepsilon_{b1} + w_c \varepsilon_{c1},\ ...] \end{aligned} \tag{6.7}$$

Here, the w values represent the weightings for the three techniques. Using this formulation, we find that the weighted-mean is:

$$\begin{aligned} \overline{x}_{SWM} &= w_a A_a + w_b A_b + w_c A_c + \frac{1}{n}\sum_{i=1}^{n}(w_a \varepsilon_{ai} + w_b \varepsilon_{bi} + w_c \varepsilon_{ci}) \\ &= w_a \overline{x}_a + w_b \overline{x}_b + w_c \overline{x}_c \end{aligned} \tag{6.8}$$

Using Equation (6.2) we can derive the variance of this SWM-distribution:

$$S^2_{SWM} = \frac{\sum_{i=1}^{n}(w_a^2 \varepsilon_{ai}^2 + w_b^2 \varepsilon_{bi}^2 + w_c^2 \varepsilon_{ci}^2 + 2w_a \varepsilon_{ai} w_b \varepsilon_{bi} + 2w_a \varepsilon_{ai} w_c \varepsilon_{ci} + 2w_b \varepsilon_{bi} w_c \varepsilon_{ci})}{n-1} \tag{6.9}$$

Assuming the errors of the distributions are random and uncorrelated, (6.9) reduces to:

$$S^2_{SWM} = \frac{\sum_{i=1}^{n}(w_a^2 \varepsilon_{ai}^2 + w_b^2 \varepsilon_{bi}^2 + w_c^2 \varepsilon_{ci}^2)}{n-1} = w_a^2 S_a^2 + w_b^2 S_b^2 + w_c^2 S_c^2 \tag{6.10}$$

From this equation, we see that the SWM-distribution has a normal distribution, and that the differences between the individual means are not a factor in the variance estimate.

If errors are correlated, (6.9) reduces to:

$$\begin{aligned} S^2_{SWM} &= w_a^2 S_a^2 + w_b^2 S_b^2 + w_c^2 S_c^2 \\ &\quad + 2w_a w_b Cov(x_a, x_b) + 2w_a w_c Cov(x_a, x_c) + 2w_b w_c Cov(x_b, x_c) \end{aligned} \tag{6.11}$$

In this expression, the covariance (*Cov*) is calculated according to:

$$Cov(x_a, x_b) = \frac{\sum_{i=0}^{n}(x_{ai} - \overline{x}_a)(x_{bi} - \overline{x}_b)}{n-1} \tag{6.12}$$

It is also useful to express (6.11) in terms of correlation coefficients ($r_{a,b}$). In this form, (6.11) is written

$$S_{SWM}^2 = w_a^2 S_a^2 + w_b^2 S_b^2 + w_c^2 S_c^2 + 2w_a S_a w_b S_b r_{a,b} + 2w_a S_a w_c S_c r_{a,c} + 2w_b S_b w_c S_c r_{b,c} \quad (6.13)$$

When combining estimates, it is important to examine how errors could be correlated. An example of this correlation is found when calculating CFC-11 loss rates. In this case, errors associated with photolysis would be correlated between the satellite estimate and the model estimate. Also note that the total variance of the J-distribution depends on the correlation sign - an anti-correlation reduces the variance since errors between two estimates would tend to cancel each other.

Using the example shown in Figure 6.A1 we can test the concept as follows. The weighting factor is defined to be proportional to the inverse of the standard deviation, i.e., $w_a \propto 1/S_a$, $w_b \propto 1/S_b$, and $w_c \propto 1/S_c$ (normalized to sum to a value of 1). Taking the obviously "non-normal" J-distribution in Figure 6.A1, we randomly select "measurements" from each of the three distributions and average those three measurements multiple times using the adopted weighting. Figure 6.A2 shows the distribution of these multiple 3-point averages. The distribution shown in Figure 6.A2 (as predicted) is normally distributed (with the 3rd and 4th moments ~ 0). Since we did not make any assumption about the covariance among the three methods, the estimated variance of this distribution is exactly as predicted from (6.10).

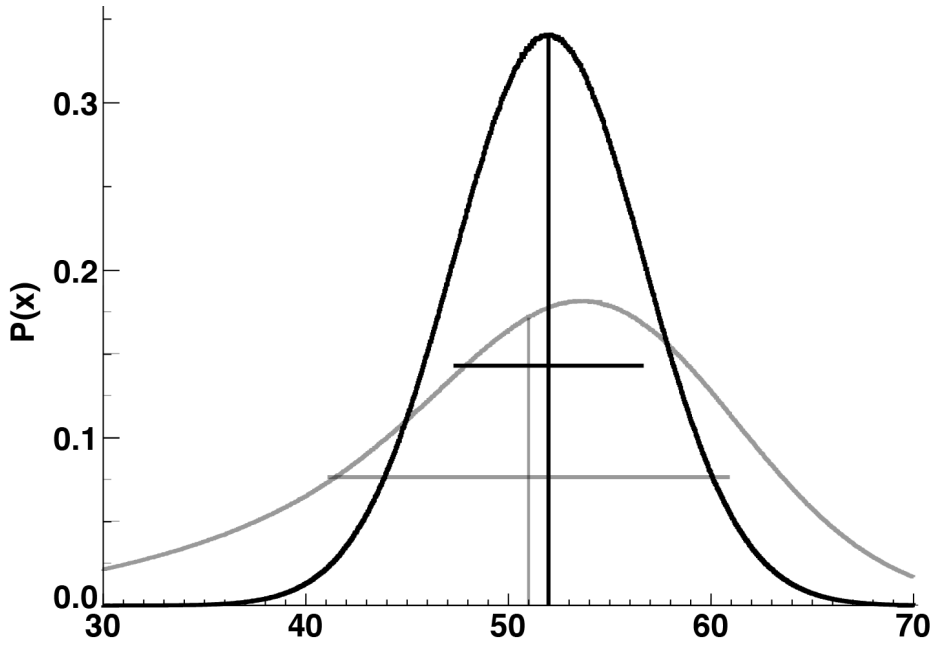

Figure 6.A2. The normal distribution of the variances from the SWM-distribution of the weighted mean. The J-distribution graph from Figure 6A-1 is included in grey for comparison. The mean of this weighted distribution is 52 (vertical line), and the standard deviation is 4.7 (horizontal line).

Conclusions

The J-distribution and the SWM-distributions provide techniques for deriving the mean and uncertainties of our observational estimates. Equation (6.6) provides a liberal or "possible" estimate of the uncertainty of the lifetimes, while Equation (6.11) provides a tight estimate yielding a "most likely" estimate. This derivation is based upon the assumptions that: 1) the errors are reasonable representations of the distributions for large numbers of sample estimates, and 2) the errors are relatively normally distributed..

For the J-distribution we use Equation (6.6) and refer to this $\pm 2\sigma$ as the "possible range" around the arithmetic mean. For the SWM-distribution we use Equation (6.11) and refer to this $\pm 2\sigma$ as the "most likely" range around the weighted mean. These equations are used to calculate of the uncertainties given in Table 6.1.

Reference

Wilks, D. S., *Statistical Methods in the Atmospheric Sciences: An Introductio*n, Academic Press, San Diego, CA, pp. 467, 1995.